Molecular Medicine in Practice

Molecular Cancer Therapeutics

A Novel, Selective Inhibitor of Fibroblast Growth Factor Receptors That Shows a Potent Broad Spectrum of Antitumor Activity in Several Tumor Xenograft Models

Genshi Zhao[1], Wei-ying Li[1], Daohong Chen[1], James R. Henry[2], Hong-Yu Li[2], Zhaogen Chen[2], Mohammad Zia-Ebrahimi[2], Laura Bloem[3], Yan Zhai[3], Karen Huss[3], Sheng-bin Peng[1], and Denis J. McCann[4]

Abstract

The fibroblast growth factor receptors (FGFR) are tyrosine kinases that are present in many types of endothelial and tumor cells and play an important role in tumor cell growth, survival, and migration as well as in maintaining tumor angiogenesis. Overexpression of FGFRs or aberrant regulation of their activities has been implicated in many forms of human malignancies. Therefore, targeting FGFRs represents an attractive strategy for development of cancer treatment options by simultaneously inhibiting tumor cell growth, survival, and migration as well as tumor angiogenesis. Here, we describe a potent, selective, small-molecule FGFR inhibitor, (R)-(E)-2-(4-(2-(5-(1-(3,5-Dichloropyridin-4-yl)ethoxy)-1H-indazol-3yl)vinyl)-1H-pyrazol-1-yl)ethanol, designated as LY2874455. This molecule is active against all 4 FGFRs, with a similar potency in biochemical assays. It exhibits a potent activity against FGF/FGFR-mediated signaling in several cancer cell lines and shows an excellent broad spectrum of antitumor activity in several tumor xenograft models representing the major FGF/FGFR relevant tumor histologies including lung, gastric, and bladder cancers and multiple myeloma, and with a well-defined pharmacokinetic/pharmacodynamic relationship. LY2874455 also exhibits a 6- to 9-fold *in vitro* and *in vivo* selectivity on inhibition of FGF- over VEGF-mediated target signaling in mice. Furthermore, LY2874455 did not show VEGF receptor 2–mediated toxicities such as hypertension at efficacious doses. Currently, this molecule is being evaluated for its potential use in the clinic. *Mol Cancer Ther; 10(11); 2200–10. ©2011 AACR.*

Introduction

There exist 4 different fibroblast growth factor (FGF) receptors (FGFR) in the cell: FGFR1, FGFR2, FGFR3, and FGFR4 (1). FGFR signaling activity is mediated through FGFs, their natural ligands (2). The binding of FGF to FGFR leads to the receptor dimerization and subsequent activation of downstream signaling pathways. Activated FGFR stimulates tyrosine phosphorylation and activation of a number of signaling molecules including FGFR substrate 2 (FRS2; refs. 1, 3). The phosphorylation of FRS2 leads to activation of the Grb2/Sos1 complex and subsequent activation of the mitogen-activated protein kinase pathway (3, 4). This signaling pathway contributes to FGFR-mediated cell proliferation and migration (1, 5). The activation of the FRS2 downstream pathway, phosphoinositide 3-kinase pathway, is involved in cell motility (6) and survival (1). Thus, the FGF/FGFR signaling pathway is important for many biological processes critical to tumor cells.

Aberrant regulation of the FGF/FGFR pathway has been implicated in many forms of human malignancies. FGFR and FGF are often overexpressed in numerous cancers, and their expression correlates with poor prognosis (7–13). Activating mutations in the FGFR kinase domain have been found in several types of tumors including breast, bladder, gastric, prostate, colon, multiple myeloma, and non–small cell lung carcinoma (NSCLC; refs. 5, 12). Genomic amplification of *FGFR* locus has also been detected in patients with breast, gastric, and lung cancers and multiple myeloma (5, 10–12). Overexpression of FGFR or FGF has also been found in many different types of tumors including bladder, prostate, and lung cancers and multiple myeloma (5, 12–15) and leads to tumor formation in animals (16–18). Cell lines that ectopically overexpress FGF or FGFR display transformed phenotype and grow as tumors in nude mice (12, 16–21). In addition to their roles in tumor formation and progression, FGF and FGFR also act as key regulators of angiogenesis (2, 22–24), especially during

Authors' Affiliations: [1]Cancer Research, [2]Medicinal Chemistry, [3]Lead Optimization Biology, and [4]Drug Disposition, Lilly Research Laboratories, Eli Lilly and Company, Indianapolis, Indiana

Corresponding Author: Genshi Zhao, Cancer Research, DC0434, Lilly Research Laboratories, Eli Lilly and Company, Indianapolis, IN 46285. Phone: 317-276-2040; Fax: 317-276-1414; E-mail: Zhao_Genshi@Lilly.com

doi: 10.1158/1535-7163.MCT-11-0306

tumor growth. Upregulation of FGF/FGFR signaling activity also leads to resistance to antiangiogenic and other chemotherapies (12, 25–28). Together, the FGF/FGFR pathway is essential to cancer cells, and inhibition of this pathway therefore offers potential clinical utilities for treating various types of cancers.

Many of the published FGFR inhibitors retain significant activity against VEGF receptor 2 (VEGFR2; refs. 29–31). VEGF/VEGFR2-based antiangiogenic therapies are approved for the treatment of several types of cancers (26, 32, 33). However, the antiangiogenic therapies are associated with side effects such as hypertension and bleeding (34–37). FGFR signaling plays a functional role in specific tumor types as well as in their angiogenesis. To avoid the side effects of the antiangiogenic therapies, we sought to develop an orally bioavailable, FGFR-dominant kinase inhibitor lacking significant activity against VEGFR2 *in vivo*. To this end, we developed a potent FGFR inhibitor, LY2874455, that shows robust dose-dependent efficacy in multiple preclinical tumor models. Therefore, LY2874455 exhibits a potential clinical use for treating various forms of human malignancies.

Materials and Methods

Biochemical filter-binding assays for detection of FGFR phosphorylation activities

Reaction mixtures contained 8 mmol/L Tris-HCl (pH 7.5), 10 mmol/L HEPES, 5 mmol/L dithiothreitol, 10 μmol/L ATP, 0.5 μCi ^{33}P-ATP, 10 mmol/L $MnCl_2$, 150 mmol/L NaCl, 0.01% Triton X-100, 4% dimethyl sulfoxide, 0.05 mg/mL poly(Glu:Tyr) (4:1, average molecular weight of 20–50 kDa; Sigma), and 7.5, 7.5, and 16 ng of FGFR1, FGFR3, and FGFR4, respectively, and were incubated at room temperature for 30 minutes followed by termination with 10% H_3PO_4. The reaction mixtures were transferred to 96-well MAFB filter plates that were washed 3 times with 0.5% H_3PO_4. After air-drying, the plates were read with a Trilux reader.

Cell-based Acumen and AlphaScreen SureFire assays for detection of FGF9- and FGF2-induced extracellular signal-regulated kinase phosphorylation in bladder cancer and human umbilical vein endothelial cell cells, respectively

All cell lines used in this article were not authenticated. After overnight growth, RT-112 cells (DSMZ) were washed, incubated in RPMI 16409 containing 20 mg/mL bovine serum albumin (BSA) at 37°C for 3 hours, and treated with LY2874455 at 37°C for 1 hour followed by the addition of FGF9 (500 ng/mL; R&D Systems) for 20 minutes. The plates were fixed with formaldehyde (3.7%) followed with washing 3 times with PBS and incubation with cold methanol at −20°C for 30 minutes. The plates were washed 3 times with PBS and incubated at 4°C overnight with shaking. After the addition of phosphorylated extracellular signal-regulated kinase (p-Erk) antibody (Cell Signaling), the plates were incubated at room temperature for 1 hour, washed, and then incubated with Alexa Fluor 488 (Invitogen). The plates were read after the addition of propidium iodide with an Acumen Explorer (TTP LabTech).

After overnight growth in endothelial basal medium, human umbilical vein endothelial cells (HUVEC) were washed and incubated in the same medium (1.5% serum and 20 mg/mL BSA) at 37°C/5% CO_2 for 3 hours. The plates were incubated for 1 hour after the addition of LY2874455 and then FGF2 (50 ng/mL, Sigma) for 15 minutes. After removing the medium and adding a lysis buffer (TGR Biosciences), the plates were incubated at room temperature for 10 minutes with shaking. The lysates were transferred to a 384-well plate (Nunc) filled with 10 μL of reaction mixture (TGR Biosciences). The plates were sealed, incubated at room temperature for 2 hours, and read with an EnVision06 reader.

FGF2- and VEGF-induced tube formation assays

After overnight growth in MCDB-131 (Invitrogen), adipose-derived stem cells (50,000 per well) and human erythroid colony-forming cells (5,000 per well) were incubated at 37°C for 3 to 4 hours. Then, FGF2 or VEGF (50 ng/mL each; Biosource) was added followed by the addition of LY2874455. After incubation at 37°C for 4 days, the medium was removed and ice-cold 70% ethanol was added followed by washing 3× with PBS at room temperature for 20 minutes. The plates were incubated at 37°C for 1 hour after the addition of the antibody against the human CD31 (R&D Systems) and washed 3× with PBS followed by the addition of the antibody against smooth muscle actin labeled with Cy3 (Sigma). The plates were incubated at room temperature for 1.5 hours and washed 3× with PBS followed by the addition of Alex Fluor-488 donkey anti-sheep IgG secondary antibody and Hoechst in PBS. The plates were incubated at room temperature for 30 minutes, washed 3× with PBS, and read using an ArrayScan reader.

MSD ELISA–based detection of phosphorylated FRS2 in cancer cells

SNU-16 and KATO-III (KCLB) cells after grown in RPMI 1640 overnight were treated with LY2874455 at 37°C for 1 hour. After removing the medium, cells were lysed (MSD lysis buffer). After centrifugation, the supernatant was collected. The detection of phosphorylated FRS2 (p-FRS2) was carried out according to the manufacturer's recommendations.

Western blot assay for detection of phosphorylated FGFR2in gastric cancer cells

SNU-16 and KATO-III cells were grown, treated, and processed as described earlier. The resulting lysates were analyzed by SDS-PAGE. After the transfer, the nitrocellulose membrane was blocked with TBS buffer (5% dry milk) and phosphorylated FGFR (p-FGFR) antibody (Cell Signaling). The membrane was blocked with a horseradish peroxidase–conjugated secondary antibody

(Cell Signaling) in TBS (5% BSA), developed in Super-Signal Western Pico Chemiluminescent Substrate (Pierce), and exposed to a Biomax Xar film (Kodak).

The preparation of SNU-16 tumor xenograft lysates was the same as described earlier for p-FRS2. The level of p-FGFR in tumors was detected as described earlier for detecting p-FGFR from KATO-III and SNU-16 cancer cell lines.

Cell proliferation assay

Cells (2,000 per well) were first grown in RPMI for 6 hours and treated with LY2874455 at 37°C for 3 days. The cells were stained at 37°C for 4 hours and then solubilized at 37°C for 1 hour. Finally, the plate was read at 570 nm using a plate reader (Spectra Max Gemini XS).

MSD-based *in vivo* target inhibition assays for measuring FGF2-induced Erk and VEGF-induced VEGFR2 phosphorylation in mouse heart tissues and also p-FRS2 in tumors

Female nude mice (CD-1 nu/nu) were acclimated for 1 week before treatment. Animals were administered with LY2874455 formulated in 10% *Acacia* by oral gavage. Two hours after dosing, the animals were intravenously injected with mouse FGF2 (6 μg per animal; Biosource) and sacrificed 10 minutes after injection. Animal heart was homogenized in cold lysis buffer (Boston BioProduct) containing phosphatase inhibitors (Sigma). After centrifugation, the supernatants were collected and analyzed by MSD phospho-Erk ELISA (MSD) to determine tissue p-Erk level. The inhibitory activity of LY2874455 against VEGFR2 was assessed as described earlier except VEGF (6 μg per animal; R&D Systems) and MSD phospho-Kdr ELISA (MSD) were used. The ELISA procedures were the same per manufacturer's recommendation (MSD) except that 0.2% SDS is added to the lysis buffer. TED_{50} (or TEC_{50}) and TED_{90} (or TEC_{90}) were defined as the dose or the concentration necessary to achieve 50% and 90% inhibition at this time point, respectively.

SNU-16 and OPM-2 tumor xenograft tissues were homogenized in a Tris lysis buffer (MSD) containing beads (MP Biomedicals). The lysate preparation and p-FRS2 determination were carried out as described earlier.

To determine compound exposure, plasma samples were prepared and analyzed with a liquid chromatography/mass spectrometer–mass spectrometer system (Applied Biosystems). Pharmacokinetic parameters were calculated with Watson LIMS information management system (Thermo Electron).

Assessment of effects on blood pressure

Four male rats (Sprague Dawley CD/IGS) per group were dosed with vehicle (1% hydroxyethylcellulose, 0.25% polysorbate 80, and 0.05% Dow Corning antifoam 1510-US in purified water) on day 1 and LY2874455 (1, 3, and 10 mg/kg) on day 0. On day 1, at least 120 minutes of control data were collected following vehicle administration. On day 0, data were collected for approximately 20 hours beginning after the last animal was dosed.

Tumor xenograft models for assessing efficacy of LY2874455

RT-112, OPM-2 (DSMZ), SNU-16, and NCI-H460 cells (American Type Culture Collection) were grown as described earlier. The cells (RT-112: 2×10^6 per animal; OPM-2: 10^7 per animal; SNU-16: 10^6 per animal; and NCI-H460: 3×10^6 per animal) were mixed with Matrigel (1:1) and implanted subcutaneously into the rear flank of the mice (female, CD-1 nu/nu from Charles River Laboratories for RT-112, OPM-2, and NCI-H460 cells and female, severe combined immunodeficient from Charles River for SNU-16 cells). The implanted tumor cells grew as solid tumors. To test the efficacy of LY2874455 in these models, the animals were orally dosed with approximately 1 mg/kg (TED_{50}) or 3 mg/kg (TED_{90}) of LY2874455 in 10% *Acacia* once (every day) or twice a day after tumors reached approximately 150 mm^3. The tumor volume and body weight were measured twice a week.

Results

Discovery of LY2874455

LY2874455, (*R*)-(*E*)-2-(4-(2-(5-(1-(3,5-dichloropyridin-4-yl)ethoxy)-1*H*-indazol-3yl)vinyl)-1*H*-pyrazol-1-yl)ethanol, is a type I pan-FGFR kinase inhibitor (Fig. 1A). On the basis of the X-ray crystal structures obtained on structurally related compounds bound to the FGFR3 protein kinase domain construct (Fig. 1B), the core indazole binds in the ATP pocket and forms key hydrogen bonds with the carbonyl of glutamate 230 (2.9 Å) and the NH of alanine 232 (3.1 Å). The vinyl pyrazole moiety extends from the indazole 3-position toward solvent, making important hydrophobic interactions. The benzylic ether extends down into a hydrophobic pocket making a hydrogen bond between the pyridyl N and asparagine 236 (3.1 Å), with the chiral benzylic methyl group appearing to reinforce the preferred conformation. This model suggests that LY2874455 is likely an ATP-competitive type of molecule that inhibits FGFR activity via its occupation of the ATP-binding pocket of the enzyme. Consistent with this, biochemical and cellular studies show that LY2874455 indeed inhibits FGFR autophosphorylation activity (see later).

Biochemical characterization of the purified FGFR proteins and the inhibitor LY2874455

To assess the ability of LY2874455 to inhibit FGFRs, we cloned the cDNA corresponding to the cytoplasmic/kinase domain of each human *fgfr* gene, expressed their gene products in SF9 insect cells as N-terminal His-tagged proteins, FGFR1 [amino acids (aa) 406–822], FGFR2 (aa 407–821), FGFR3 (aa 405–806); and FGFR4 (aa 399–802), and purified the proteins to apparent homogeneity by immobilized metal affinity chromatography followed

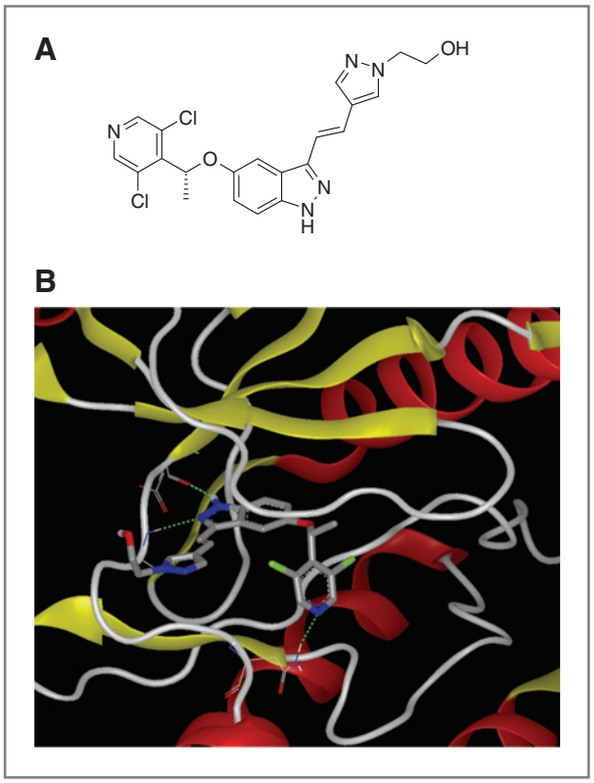

Figure 1. A, chemical structure of LY2874455, (R)-(E)-2-(4-(2-(5-(1-(3,5-Dichloropyridin-4-yl)ethoxy)-1H-indazol-3yl)vinyl)-1H-pyrazol-1-yl)-ethanol. B, a binding model of LY2874455 in the ATP site of FGFR3.

by size-exclusion chromatography (data not shown). We then developed a filter-binding assay for each purified protein. These assays, using poly(Glu:Tyr) and ^{33}P-labeled ATP as substrates, measure autophosphorylation and phosphate-transferring activities of each enzyme (Materials and Methods). Using these assays, we kinetically characterized each FGFR. We showed that the purified FGFR1, 2, 3, and 4 proteins had the K_M values of 37.1, 47.1, 123.8, and 167 μg/mL for poly(Glu:Tyr), respectively, which correspond to 0.74–1.85, 0.94–2.35, 2.48–6.19, and 3.34–8.35 μmol/L, respectively, because the poly(Glu:Tyr) have an average molecular weight of 20 to 50 kDa (Sigma). Next, we determined the K_M values of FGFR1, 2, 3, and 4 proteins for ATP to be 36.7, 10.2, 59.9, and 12.3 μmol/L, respectively.

To determine its inhibitory activity, we tested LY2874455 in the filter-binding assays developed. We showed that LY2874455 inhibited FGFR1, 2, 3, and 4 in a dose-dependent manner, with IC_{50} values of 2.8, 2.6, 6.4, and 6 nmol/L, respectively. Thus, these biochemical results suggest that LY2874455 is a pan-FGFR inhibitor with a similar potency for each enzyme.

To assess its biochemical selectivity, LY2874455 was tested in a VEGFR2 time-resolved fluorescence resonance energy transfer assay (CEREP). LY2874455 seemed to inhibit VEGFR2, with an IC_{50} of approximately 7 nmol/L. Because this assay uses a universal artificial peptide substrate and a truncated VEGFR2 enzyme with its cytoplasmic domain deleted (CEREP), the selectivity of LY2874455 against VEGFR2 was further assessed by the cellular and *in vivo* assays (see later).

Cellular activity of LY2874455

On the basis of the biochemical results, LY2874455 seems to be a potent pan-inhibitor of FGFRs. To assess its ability to inhibit the target in the cell, we attempted to develop cell-based assays that directly measure the inhibition of FGFR phosphorylation in the cell. However, our extensive efforts toward developing these types of p-FGFR assays failed because of the lack of high-quality antibodies against p-FGFRs. We next explored the possibility of developing assays that can measure the inhibition of the downstream signaling activity of FGFR. To this end, we developed 2 high-throughput cellular assays that measure the inhibition of FGF2- and FGF9-induced Erk phosphorylation in HUVECs and RT-112 cells, respectively (Materials and Methods). The HUVECs and RT-112 cell lines are shown to express FGFR1 (data not shown; ref. 2) and FGFR3 (38), respectively. Using these assays, we showed that LY2874455 potently inhibited the Erk phosphorylation induced by FGF2 and FGF9 in both cell lines in a dose-dependent manner, with average IC_{50} values of 0.3 to 0.8 nmol/L (Fig. 2A). To establish that the inhibition of Erk phosphorylation by LY2874455 is due to its inhibition of FGFR in the cell, we tested this molecule in 2 gastric cancer cell lines, SNU-16 and KATO-III, which contain a high level of p-FGFR2 due to the amplification of *fgfr2* in the cells (8, 39). LY2874455 indeed inhibited FGFR2 phosphorylation in SNU-16 and KATO-III cells, with estimated IC_{50} values of 0.8 and1.5 nmol/L, respectively (Fig. 2B). In addition, LY2874455 inhibited the phosphorylation of FRS2, an immediate downstream target of FGFR in these cell lines, again with a similar potency of 0.8 to 1.5 nmol/L (Fig. 2C). Together, these results suggest that LY2874455 inhibits FGFR in the cell.

To further establish that LY2874455 specifically inhibits FGFR in the cell, we tested this molecule in a cell proliferation assay to assess its ability to inhibit different multiple myeloma cancer cell lines, some of which (KMS-11 and OPM-2 cells) carry an FGFR3 chromosomal translocation, resulting in the overexpression of FGFR3 (40, 41). In this study, we also used L-363 and U266, known to contain little or no FGFR3 (41). We confirmed by a Western blot analysis that KMS-11 and OPM-2 cells, but not L-363 and U266 cells, contained a relatively high level of p-FGFR (data not shown). The relative IC_{50} values of LY2874455 for KMS-11, OPM-2, L-363, and U266 cells were determined to be 0.57, 1.0, 60.4, and 290.7 nmol/L, respectively. Thus, the presence of the FGFR3 chromosomal translocation in multiple myeloma cancer cell lines renders them significantly more susceptible to inhibition by LY2874455. Consistent with this finding, we have also shown that the presence of *fgfr2* amplification in gastric

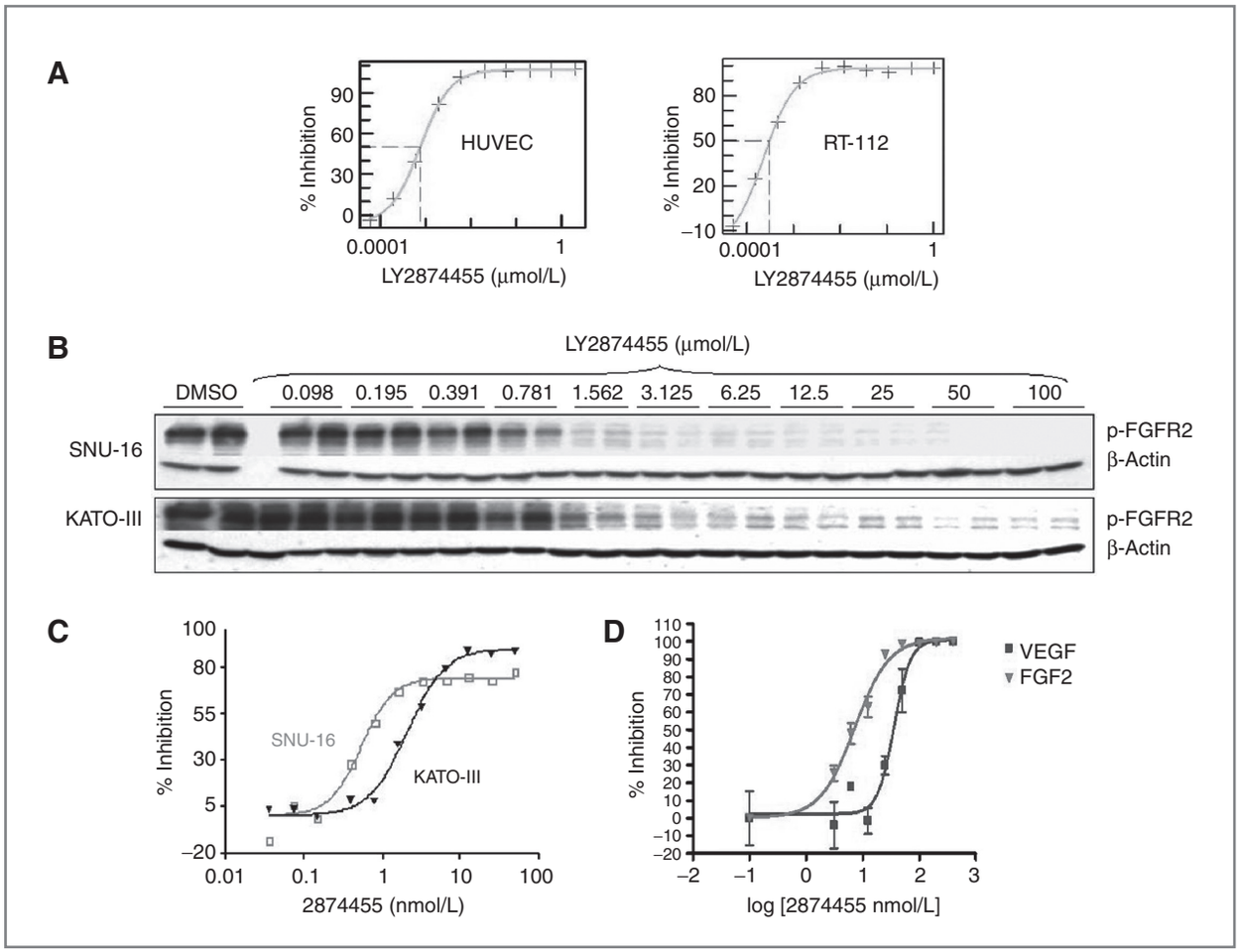

Figure 2. Inhibition of FGF/FGFR- and VEGF/VEGFR2-mediated signaling activities in cells by LY2874455. RT-112 cells, HUVECs, KATO-III cells, and SNU-16 cells were grown and treated with LY2874455 at various concentrations (Materials and Methods). After the treatment, cells were processed and analyzed for p-Erk, p-FGFR2, and p-FRS2 levels (Materials and Methods). Adipose-derived stem cells and human erythroid colony-forming cells were grown, induced with FGF2 or VEGF, and treated with LY2874455 at various concentrations (Materials and Methods). After the treatment, tubes formed were visualized and quantified. A, inhibition of FGF2- and FGF9-induced Erk phosphorylation in HUVECs and RT-112 cells. B, inhibition of FGFR2 phosphorylation in SNU-16 and KATO-III cells. DMSO, dimethyl sulfoxide. C, inhibition of p-FRS2 in SNU-16 and KATO-III cells. D, inhibition of FGF2 (▼)- or VEGF (■)- induced tube formation.

cancer cell lines renders them significantly more susceptible to inhibition by LY2874455 than those with little or no FGFR2. For example, SNU-16 and KATO-III with a highly amplified *fgfr2* are more than 1,000-fold sensitive to inhibition by LY28774455 than NUGC-3 and SH-10-TC in which no *fgfr2* amplification was observed (data not shown). Therefore, these results suggest that LY2874455 inhibits FGFR in the cell and that its antiproliferative effects are directly linked to the inhibition of FGFR signaling.

Several reported FGFR inhibitors have a dominant activity against VEGFR2 as compared with FGFRs (29–31). At efficacious doses, these molecules also retain many of the class effects associated with VEGFR2/VEGFR blockade including hypertension and bleeding (34–37). We therefore wanted to further assess LY2874455 with regard to its cellular and *in vivo* selectivity toward FGFRs versus VEGFR2. Using the FGF2- and VEGF-induced tube formation assays, we evaluated the ability of LY2874455 to inhibit these growth factor–induced tube-forming activities. As shown in Fig. 2D, LY2874455 inhibited the FGF2- and VEGF-induced tube-forming activities, with IC_{50} values of 0.6 and 3.6 nmol/L, respectively. Thus, these results show that LY2874455 is significantly more potent (≈6-fold) at inhibiting the FGF2- than VEGF-induced tube-forming activity. This finding is further confirmed by the results of the *in vivo* target inhibition (IVTI) and toxicology studies (see later).

IVTI activity of LY2874455

On the basis of the cellular assay results that LY2874455 seems to be a potent and selective FGFR inhibitor, we want to further confirm that this molecule inhibits the target in an *in vivo* setting. As discussed earlier, because

of the lack of high-quality antibodies against p-FGFR that could be used for cellular assay development, we ruled out the possibility of developing an IVTI assay that directly measured FGFR phosphorylation in animal tissues. To this end, we explored several alternative approaches including the development of an assay based on the detection of the downstream signaling molecules of FGFR, and subsequently developed for the first time a robust IVTI assay that measures FGF-stimulated Erk phosphorylation in the heart tissues of mice (Materials and Methods). Using this assay, we showed that LY2874455 exhibited a potent, dose-dependent inhibition of FGF-induced Erk phosphorylation in the heart tissues of mice with estimated TED_{50} and TED_{90} values of 1.3 and 3.2 mg/kg, respectively (Fig. 3A). In this study, we also examined the relationship between the exposures or concentrations of LY2874455 in the plasma and the inhibition of Erk phosphorylation. The results of this study showed that LY2874455 also exhibited a concentration-dependent inhibition of FGF-induced Erk phosphorylation, with estimated TEC_{50} and TEC_{90} values of 6.2 and 28.4 nmol/L, respectively (Fig. 3B). To assess the *in vivo* stability of this molecule, LY2874455 was tested in mice at 3 mg/kg (TED_{90}). This molecule inhibited 99.7%, 95.5%, 76.9%, 45.3%, and −23.3% of FGF-induced Erk phosphorylation 1, 2, 4, 8, and 24 hours, respectively, after dosing (data not shown). Finally, to further confirm these mouse IVTI findings, we tested LY2874455 in a rat heart IVTI assay. Consistent with the results obtained from the mouse IVTI assay, LY2874455 also exhibited a potent IVTI activity with an estimated TED_{50} of 0.39 mg/kg (data not shown). Together, the results of these studies show that LY2874455 potently inhibits the FGFR signaling activity *in vivo*. These findings were further confirmed by the results of the *in vivo* efficacy and toxicity studies (see later).

On the basis of its differential inhibition of FGF- and VEGF-induced tube-forming activities, we wanted to further assess the VEGFR2 selectivity of LY2874455 *in vivo*. To this end, we also developed an IVTI assay that measures the VEGF-induced VEGFR2 phosphorylation in the heart tissues of mice (Materials and Methods).

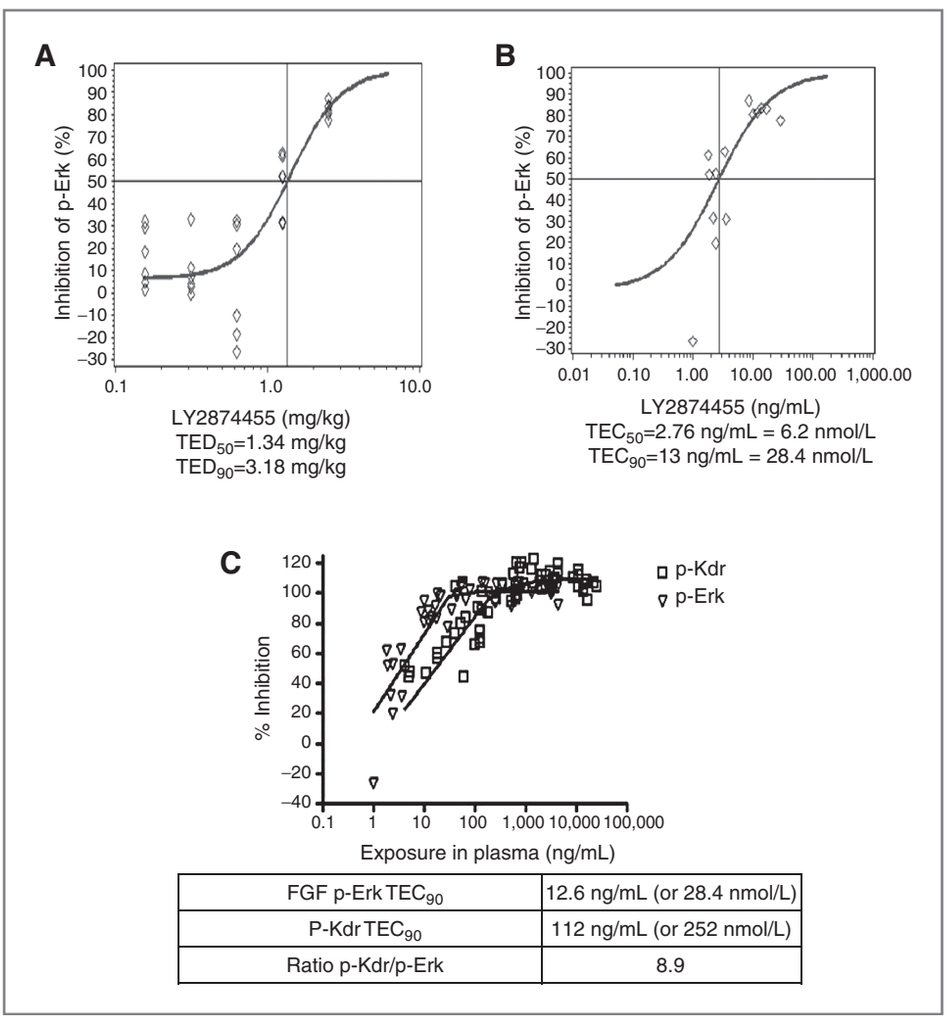

FGF p-Erk TEC_{90}	12.6 ng/mL (or 28.4 nmol/L)
P-Kdr TEC_{90}	112 ng/mL (or 252 nmol/L)
Ratio p-Kdr/p-Erk	8.9

Figure 3. Inhibition of FGF- and VEGF-induced Erk and VEGFR2 phosphorylation, respectively, in mouse heart tissues by LY2874455. Mice were first treated with LY2874455 at various doses followed by tail vein injection of mouse FGF2 or VEGF (Materials and Methods). After the FGF2 or VEGF treatment, the heart tissues were collected and processed for the analysis of p-Erk and p-VEGFR2 levels by MSD ELISA assays (Materials and Methods). The plasma was also collected for the analysis of the exposures or concentrations of LY2874455 versus p-Erk or p-VEGFR2 levels (Materials and Methods). A, dose-dependent inhibition of p-Erk formation. B, exposure-dependent inhibition of p-Erk formation. C, overlay of exposures versus inhibition of p-Erk and p-VEGFR2 formation.

When tested in this assay (Fig. 3C), LY2874455 exhibited a concentration-dependent inhibition of VEGFR2 phosphorylation with estimated TEC_{50} and TEC_{90} values of 36 and 252 nmol/L, respectively, as compared with the TEC_{50} (6.2 nmol/L) and TEC_{90} (28.4 nmol/L) obtained in the FGF-induced Erk phosphorylation assay. The results of this study show that LY2874455 is again much more (6- to 9-fold) potent at inhibiting the FGF- than VEGF-induced signaling activity *in vivo* (i.e., VEGF p-VEGFR2 TEC_{50}/FGF p-Erk TEC_{50} = 36 nmol/L/6.2 nmol/L ≈ 6; and VEGF p-VEGFR2 TEC_{90}/FGF p-VEGFR2 TEC_{90} = 252 nmol/L/28.4 nmol/L ≈ 9).

VEGF/VEGFR2-based antiangiogenic therapies are associated with hypertension in the clinical setting (34–37). We therefore wanted to further assess whether treatment of animals with LY2874455 could also lead to a dose-dependent increase in blood pressure. When rats were dosed with LY2874455 at 1 and 3 mg/kg, which is 2.6- and 7.7-fold over the TED_{50} (0.39 mg/kg) obtained in the rat heart IVTI assay, respectively, there were no significant changes observed in blood pressure (Fig. 4A and B). However, when rats were dosed with LY2874455 at 10 mg/kg, which is 25.6-fold over the TED_{50}, there were significant increases observed in arterial pressures (Fig. 4C). The peak of this increase in blood pressure occurred approximately between 4 and 8 hours after dosing (Fig. 4C). These results suggest that the VEGFR2 activity was inhibited *in vivo* by LY2874455 at 10 mg/kg but not at 1 and 3 mg/kg. Therefore, a treatment based on this molecule may avoid the class effects of the anti-VEGF/VEGFR2-based therapies in the clinic. Taken together, these *in vivo* and *in vitro* studies establish that LY2874455 is a potent FGFR-dominant inhibitor.

In vivo efficacy of LY2874455 in different tumor models

To assess its potential clinical utility, we evaluated the *in vivo* efficacy of LY2874455 in different tumor models that are dependent on or relevant to FGF/FGFR biology. By testing the molecule in these FGF/FGFR relevant tumor models, we also hope to identify the specific types of tumor histologies that can be effectively targeted by the molecule, thereby used as a basis for patient selection in the clinic. To this end, we identified and characterized several appropriate cancer cell lines with altered FGFR or FGF levels, RT-112 (overexpressing FGFR3; ref. 38), SNU-16 (amplified FGFR2; ref. 39), OPM-2 (overexpressing a mutant *FGFR3* because of a chromosomal translocation; ref. 40, 41), and NCI-H460 (a high level of FGF2; ref. 42), and subsequently used these cell lines to establish tumor xenograft models for assessing efficacy of the molecule. As shown in Fig. 5, LY2874455 exhibited a rapid, robust, dose-dependent inhibition of tumor growth in all 4 models tested. Importantly, this molecule caused a significant regression of tumor growth in the RT-112, SNU-16, and OPM-2 tumor models, especially

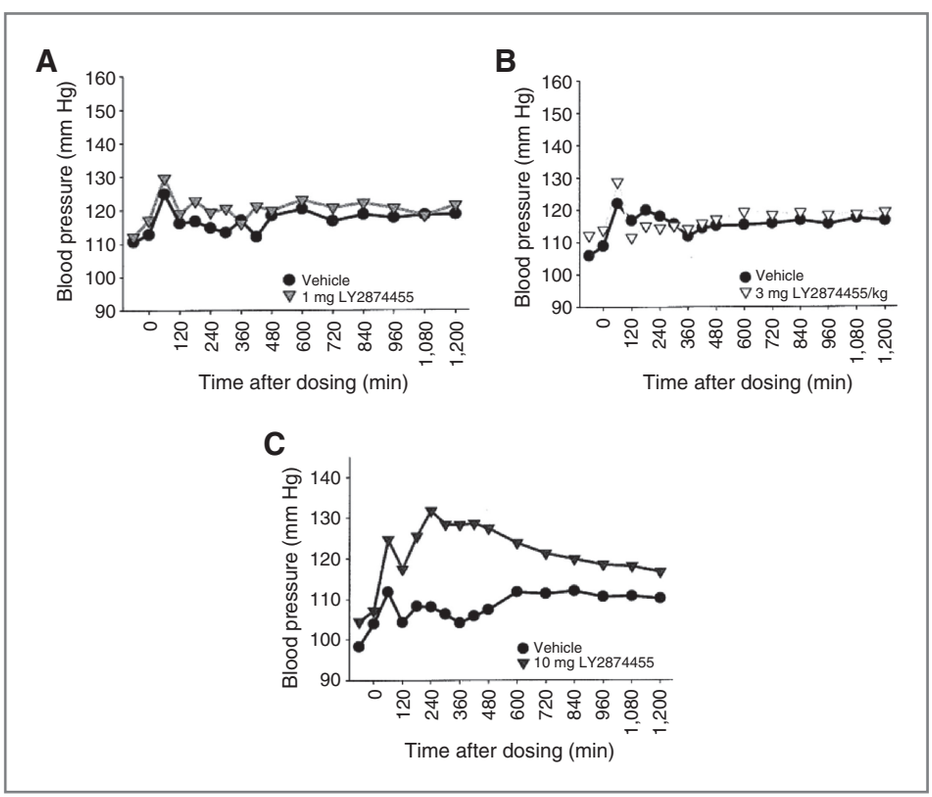

Figure 4. Effects of LY2874455 on blood pressure in rats. Animals were treated and effects on blood pressure were assessed as described in Materials and Methods. Mean arterial blood pressure was measured in rats dosed with 1 mg/kg (A), 3 mg/kg (B), and 10 mg/kg (C) of LY2874455.

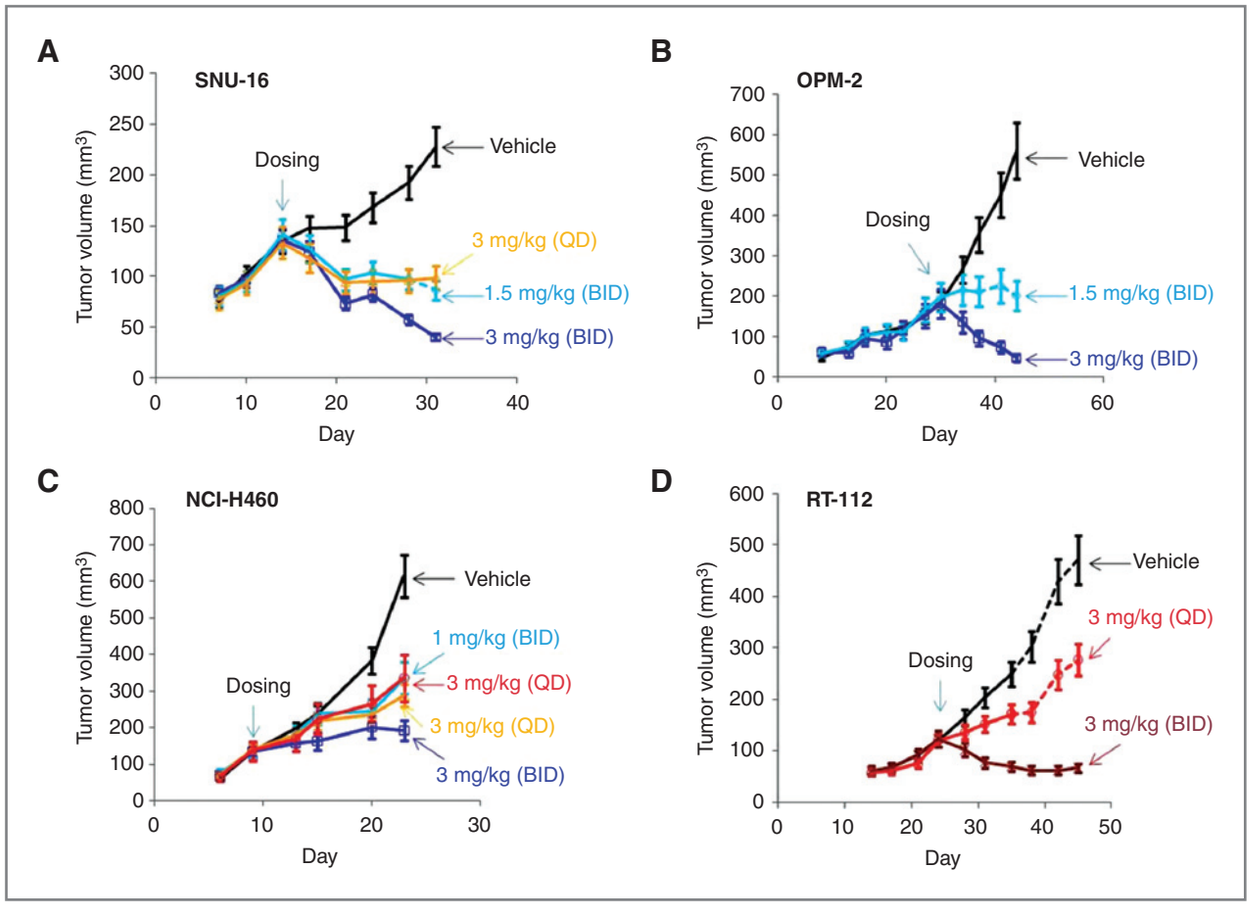

Figure 5. Efficacy of LY2874455 in different tumor xenograft models. Mice were subcutaneously implanted with SNU-16, OPM-2, NCI-H460, and RT-112 cells (Materials and Methods). Once tumors grew to about 150 mm^3, animals were randomly assigned (6–8 per group) and orally dosed with vehicle alone or LY2874455 at the indicated doses on an once or twice a day dosing schedule for 14 to 21 days (Materials and Methods). The growth of tumors was monitored and measured twice a week. A, SNU-16 tumor xenografts treated with LY2874455 (1.5 and 3 mg/kg once or twice a day). B, OPM-2 tumor xenografts treated with LY2874455 (1.5 and 3 mg/kg twice a day). C, NCI-H460 tumor xenografts treated with LY2874455 (1 and 3 mg/kg once or twice a day). D, RT-112 tumor xenografts treated with LY2874455 (3 mg/kg once or twice a day). QD, once a day; BID, twice a day.

when dosed at 3 mg/kg twice a day (Fig. 5A, B, and D). Also, LY2874455 exhibited an excellent pharmacokinetic/pharmacodynamic relationship as shown by its dose-dependent inhibition of the tumor growth at TED_{50} and TED_{90} (1 and 3 mg/kg, respectively). When tested in the RT-112 tumor xenograft model on an intermittent dosing schedule (twice a day 1 week on and 1 week off or twice a day 2 days on and 2 days off), LY2874455 was also efficacious (data not shown). Taken together, the results of these *in vivo* efficacy studies show that LY2874455 exhibits a potent broad spectrum of antitumor activity in a number of tumor models that represent the major types of tumor histologies in the clinic.

To assess whether the inhibition of tumor growth by LY2874455 is due to the inhibition of the target in the cell, we analyzed the tumor samples that had been treated with the molecule for the effects of the molecule on p-FGFR and p-FRS2 levels. LY2874455 exhibited a dose-dependent inhibition of FGFR2 phosphorylation in SNU-16 tumor xenografts as compared with that in the vehicle control tumors (Fig. 6A and B). Similarly, this molecule inhibited FRS2 phosphorylation in a dose-dependent manner (Fig. 6C). The inhibition of FGFR2 and FRS2 phosphorylation by LY2874455 is well correlated with its attenuation of tumor growth (Figs. 5A and 6). Consistent with these findings, the inhibition of FRS2 phosphorylation by LY2874455 was also observed in OPM-2 tumor xenografts, but not in the vehicle control tumors, and that this inhibition is again well correlated with its attenuation of tumor growth (data not shown). Thus, the results of these studies show that the attenuation of tumor growth by LY2874455 is most likely due to its inhibition of the FGFR signaling activity in the cell.

Discussion

In this study, we identified LY2874455 as a novel, potent FGFR inhibitor. This molecule is an FGFR-dominant inhibitor with a significantly lower VEGFR2 activity. It is much more potent at inhibiting the proliferation of

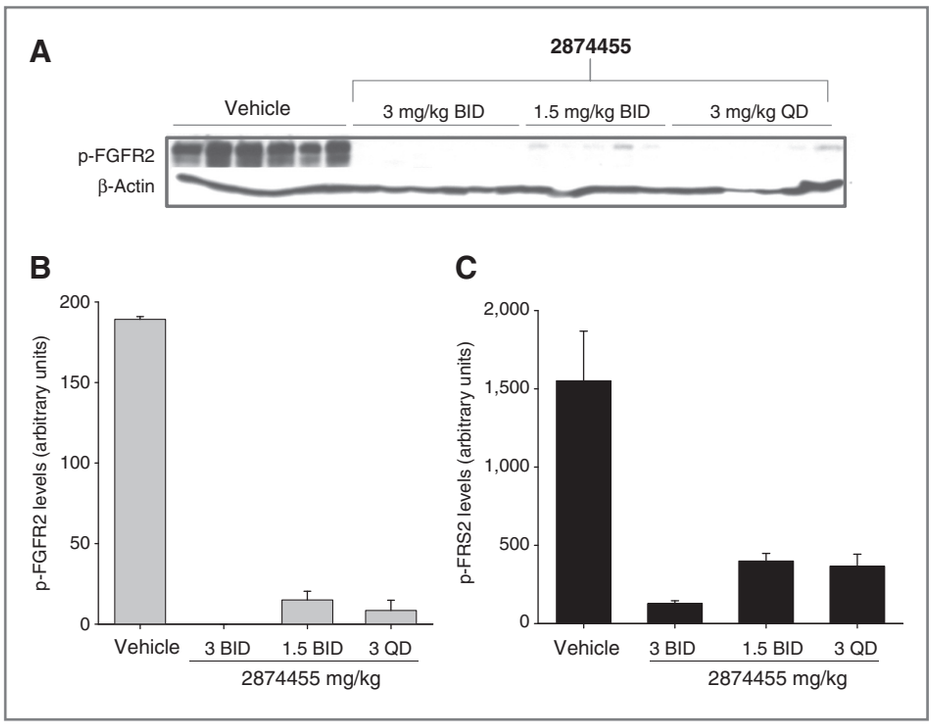

Figure 6. Inhibition of FGFR2 and FRS2 phosphorylation in SNU-16 tumor xenografts by LY2874455. After treatment with LY2874455 at various doses for about 2 weeks, the tumor xenografts derived from SNU-16 (see Fig. 5A) were collected and processed. The levels of p-FGFR2 and p-FRS2 were measured by Western blot analysis and MSD ELISA, respectively (Materials and Methods). A, Western blot analysis of p-FGFR2 levels in the tumors versus dose. B, the intensity of each band corresponding to p-FGFR2 from A was quantified and plotted versus dose. C, MSD ELISA of p-FRS2 levels in the tumors versus dose. QD, once a day; BID, twice a day.

the different cancer cell lines with increased FGF or FGFR expression than those with little or no FGFR expression. In addition, it is a potent FGFR inhibitor *in vivo* and very efficacious in several tumor models representing major tumor histologies in the clinic. Furthermore, the inhibition of the FGF/FGFR signaling pathway activity by this molecule is well correlated with its inhibition of tumor growth. Finally, this molecule does not cause significant hypertension at its efficacious dose. In light of these results, the identification of this potent FGFR-dominant inhibitor may lead to the development of novel anticancer therapies for many patients, especially those with the histologies relevant to the FGF/FGFR signaling pathway and also those in whom the anti-VEGF/VEGFR-based therapies are contraindicated.

There are several lines of evidence showing that LY2874455 inhibits the target FGFR in the cell and that this on-target inhibition leads to the robust efficacy in several FGFR relevant tumor models. First, LY2874455 is much more potent at inhibiting the proliferation of cancer cells with a significantly increased FGFR-signaling activity than those with a little or no FGFR signaling activity. Second, LY2874455 preferentially inhibits FGF- over VEGF-induced tube-forming activity. Third, LY2874455 inhibited the growth of tumor xenografts derived from gastric and multiple myeloma cell lines carrying a highly amplified FGFR2 and an overexpressed FGFR3 due to a chromosomal translocation, respectively, and this growth inhibition is correlated with its inhibition of FGFR2 and FRS2 phosphorylation in the tumor cells. Fourth, to achieve a robust antitumor activity with a VEGFR2 inhibitor, it is well established that the inhibitor has to be administered at a dose that can yield a concentration at which the target VEGFR2 activity has to be inhibited more than 90% during the period of the study (43). In our IVTI studies, we showed that LY2874455 inhibited FGFR activity by 90% but VEGFR2 activity by 45% or less (data not shown) when dosed at 3 mg/kg for 2 hours. In an IVTI time course study, LY2874455 inhibited FGFR activity by approximately 50% at 8 hours when dosed at 3 mg/kg. On the basis of these findings, it is reasonable to believe that the inhibition of VEGFR2 activity by LY2874455 would not exceed 45% at maximum, nor would last more than 4 hours (2×2) during a period of 24 hours with a twice daily dosing schedule. Furthermore, the administration of LY2874455 did not lead to a significant increase in blood pressure in rats when dosed at 1 or 3 mg/kg (2.6- and 7.7-fold over the TED_{50} of 0.39 mg/kg, respectively), but at 10 mg/kg (25.6-fold over the TED_{50} of 0.39 mg/kg). This finding again shows that LY2874455, when administrated at an efficacious dose (TED_{50} or TED_{90}), does not significantly inhibit VEGFR2 activity. Taken together, these findings indicate that the inhibition of tumor growth by LY2874455 is likely due to its inhibition of the intended target FGFR.

The importance of the FGFR signaling pathway in the pathogenesis of diverse tumor types is well documented in the clinic, as activating mutations and genomic amplification and overexpression of FGFRs or FGFs due to other genetic alterations have been reported in many different types of tumors (12). Therefore, the

development of cancer therapies based on targeting the FGF/FGFR signaling pathway represents an attractive strategy and should have broad clinical implications to the treatment of various types of cancers. In this study, we show that LY2874455 is effective at inhibiting the proliferation of a variety of different cancer cell lines, especially those with elevated FGF or FGFR levels such as gastric cancer, bladder cancer, multiple myeloma, and NSCLC cell lines. This molecule is also effective against OPM-2, which overexpresses FGFR3 and is also known to contain an activating mutation in its kinase domain (44). In addition, this molecule is potent at inhibiting the *in vivo* growth of tumor xenografts derived from these diverse cancer cell lines. In light of these findings, LY2874455 has the potential to be used as an effective anticancer agent for treating a variety of different types of cancers including, but not limited to, those as described earlier and also other types of cancers with an aberrant FGF/FGFR signaling activity. As discussed earlier, its potential clinical utilities for different types of cancer patients are currently being evaluated in a phase 1 study.

The presence of genetic alterations in or aberrant regulation of the FGFR signaling pathway also enables us to develop a robust tailoring strategy aimed at identifying and selecting appropriate patients with cancer who can most likely benefit from treatment with the molecule in the clinic. For example, patients with gastric cancers carrying an amplified *fgfr2*, which can be identified via FISH (39), are predicted to respond to treatment with LY2874455 due to the extreme sensitivity of these cell lines to the inhibition by the molecule. Likewise, patients with multiple myeloma cancers carrying an FGFR3 chromosomal translocation can also be identified via FISH (45). Finally, the finding that LY2874455 effectively inhibits FRS2 phosphorylation in tumor xenografts derived from both gastric and multiple myeloma cell lines suggests that p-FRS2 can be used as a pharmacodynamic biomarker for assessing effects of LY2874455 on its intended target in the clinic. Using well-defined patient populations in combination with the potential pharmacodynamic biomarkers may enhance the understanding of the mechanism of action of the molecule in the clinic and subsequently its clinical development.

Antiangiogenesis-based therapies are effective in the clinical setting, but they also have well-characterized side effects, limiting the duration of exposure for many patients. Furthermore, overexpression of FGF2 or alterations in other signaling pathways has been implicated in the resistance to the anti-VEGF/VEGFR2-based agents clinically and preclinically (25–27, 46). The development of the resistance could pose a challenge to the use of these therapies in the clinic (25–27, 46). As discussed earlier, although several small-molecule inhibitors of FGFR are currently in the clinical development, in general, they retain significant VEGFR2 inhibitory activity. In contrast, our molecule is predominately an FGFR inhibitor. LY2874455 may be considered for treatment of patients who progressed on anti-VEGF/VEGFR2-based therapies. Although antiangiogenic agents have shown survival benefit in both the preclinical and clinical settings, some preclinical studies have suggested that they may have the potential to accelerate tumor metastasis (47, 48). FGFR inhibitors seem to have primary effects on tumor cell growth, but they may also impact tumor-induced angiogenesis due to the important roles of FGFR in tumor and endothelial cells. This combined inhibitory effect warrants further testing in the clinic (46).

Disclosure of Potential Conflicts of Interest

No potential conflicts of interest were disclosed.

Acknowledgments

The authors thank Delu Jiang, Yan Wang, and Boyu Zhong for chemistry input and support; Xiu-Juan Yuan for help with cellular assay development; Qi Chen for computational support; Karen Britt for support on biochemical assay development; Lysiane Huber and Lisa Kays for carrying out *in vivo* studies; Yue-wei Qian and He Wang for expression and purification of FGFRs; Michelle Swearingen and Kuldeep Neote for the tube formation assays; Yong Wang for structural work; Jason Manro for statistic analysis; Jonathan Yingling, Jake Starling, and Richard Gaynor for their guidance and support; and Sandy Geeganage, Jake Starling, Robert Wild, David Monteith, Donald Thornton, Gregory D. Plowman, and Jonathan Yingling for critical review of the manuscript.

Grant Support

This work was supported by Eli Lilly and Company.

Received April 28, 2011; revised August 10, 2011; accepted September 1, 2011; published OnlineFirst September 7, 2011.

References

1. Eswarakumar VP, Lax I, Schlessinger J. Cellular signaling by fibroblast growth factor receptors. Cytokine Growth Factor Rev 2005;16:139–49.
2. Zhang X, Ibrahimi OA, Olsen SK, Umemori H, Mohammadi M, Ornitz DM. Receptor specificity of the fibroblast growth factor family. The complete mammalian FGF family. J Biol Chem 2006;281:15694–700.
3. Ong SH, Guy GR, Hadari YR, Laks S, Gotoh N, Schlessinger J, et al. FRS2 proteins recruit intracellular signaling pathways by binding to diverse targets on fibroblast growth factor and nerve growth factor receptors. Mol Cell Biol 2000;20:979–89.
4. Kouhara H, Hadari YR, Spivak-Kroizman T, Schilling J, Bar-Sagi D, Lax I, et al. A lipid-anchored Grb2-binding protein that links FGF-receptor activation to the Ras/MAPK signaling pathway. Cell 1997;89:693–702.
5. Boilly B, Vercoutter-Edouart AS, Hondermarck H, Nurcombe V, Le Bourhis X. FGF signals for cell proliferation and migration through different pathways. Cytokine Growth Factor Rev 2000;11:295–302.
6. Cross MJ, Hodgkin MN, Roberts S, Landgren E, Wakelam MJ, Claesson-Welsh L. Tyrosine 766 in the fibroblast growth factor receptor-1 is required for FGF-stimulation of phospholipase C, phospholipase D, phospholipase A(2), phosphoinositide 3-kinase and cytoskeletal reorganisation in porcine aortic endothelial cells. J Cell Sci 2000;113:643–51.

7. Cappellen D, De Oliveira C, Ricol D, de Medina S, Bourdin J, Sastre-Garau X, et al. Frequent activating mutations of FGFR3 in human bladder and cervix carcinomas. Nature Genet 1999;23:18–20.
8. Hernández S, de Muga S, Agell L, Juanpere N, Esgueva R, Lorente JA, et al. FGFR3 mutations in prostate cancer: association with low-grade tumors. Mod Pathol 2009;22:848–56.
9. Matsunobu T, Ishiwata T, Yoshino M, Watanabe M, Kudo M, Matsumoto K, et al. Expression of keratinocyte growth factor receptor correlates with expansive growth and early stage of gastric cancer. Int J Oncol 2006;28:307–14.
10. Reis-Filho JS, Simpson PT, Turner NC, Lambros MB, Jones C, Mackay A, et al. FGFR1 emerges as a potential therapeutic target for lobular breast carcinomas. Clin Cancer Res 2006;12: 6652–62.
11. Tsujimoto H, Sugihara H, Hagiwara A, Hattori T. Amplification of growth factor receptor genes and DNA ploidy pattern in the progression of gastric cancer. Virchows Arch 1997;43:383–9.
12. Turner N, Grose R. Fibroblast growth factor signalling: from development to cancer. Nat Rev Cancer 2010;10:116–29.
13. Volm M, Koomägi R, Mattern J, Stammler G. Prognostic value of basic fibroblast growth factor and its receptor (FGFR-1) in patients with non-small cell lung carcinomas. Eur J Cancer 1997;33:691–3.
14. Bergsagel PL, Kuehl WM. 2005 Molecular pathogenesis and a consequent classification of multiple myeloma. J Clin Oncol 2005;23: 6333–8.
15. Trudel S, Stewart AK, Rom E, Wei E, Li ZH, Kotzer S, et al. The inhibitory anti-FGFR3 antibody, PRO-001, is cytotoxic to t(4;14) multiple myeloma cells. Blood 2006;107:4039–46.
16. Acevedo VD, Gangula RD, Freeman KW, Li R, Zhang Y, Wang F, et al. Inducible FGFR-1 activation leads to irreversible prostate adenocarcinoma and an epithelial-to-mesenchymal transition. Cancer Cell 2007;12:559–71.
17. Memarzadeh S, Xin L, Mulholland DJ, Mansukhani A, Wu H, Teitell MA, et al. Enhanced paracrine FGF10 expression promotes formation of multifocal prostate adenocarcinoma and an increase in epithelial androgen receptor. Cancer Cell 2007;12:572–85.
18. Zhong C, Saribekyan G, Liao CP, Cohen MB, Roy-Burman P. Cooperation between FGF8b overexpression and PTEN deficiency in prostate tumorigenesis. Cancer Res 2006;66:2188–94.
19. Nomura S, Yoshitomi H, Takano S, Shida T, Kobayashi S, Ohtsuka M, et al. FGF10/FGFR2 signal induces cell migration and invasion in pancreatic cancer. Br J Cancer 2008;99:305–13.
20. Welm BE, Freeman KW, Chen M, Contreras A, Spencer DM, Rosen JM. Inducible dimerization of FGFR1: development of a mouse model to analyze progressive transformation of the mammary gland. J Cell Biol 2002;157:703–14.
21. Xian W, Schwertfeger KL, Vargo-Gogola T, Rosen JM. Pleiotropic effects of FGFR1 on cell proliferation, survival, and migration in a 3D mammary epithelial cell model. J Cell Biol 2005;171:663–73.
22. Czubayko F, Liaudet-Coopman ED, Aigner A, Tuveson AT, Berchem GJ, Wellstein A. A secreted FGF-binding protein can serve as the angiogenic switch in human cancer. Nature Med 1997;3:1137–40.
23. Kandel J, Bossy-Wetzel E, Radvanyi F, Klagsbrun M, Folkman J, Hanahan D. Neovascularization is associated with a switch to the export of bFGF in the multistep development of fibrosarcoma. Cell 1991;66:1095–104.
24. Werner S, Grose R. Regulation of wound healing by growth factors and cytokines. Physiol Rev 2003;83:835–70.
25. Batchelor TT, Duda DG, di Tomaso E, Ancukiewicz M, Plotkin SR, Gerstner E, et al. Phase II study of cediranib, an oral pan-vascular endothelial growth factor receptor tyrosine kinase inhibitor, in patients with recurrent glioblastoma. J Clin Oncol 2010;28:2817–23.
26. Bergers G, Hanahan D. Modes of resistance to anti-angiogenic therapy. Nat Rev Cancer 2008;8:592–603.
27. Casanovas O, Hicklin DJ, Bergers G, Hanahan D. Drug resistance by evasion of antiangiogenic targeting of VEGF signaling in late-stage pancreatic islet tumors. Cancer Cell 2005;8:299–309.
28. Song S, Wientjes MG, Gan Y, Au JL. Fibroblast growth factors: an epigenetic mechanism of broad spectrum resistance to anticancer drugs. Proc Natl Acad Sci U S A 2000;97:8658–63.
29. Hilberg F, Roth GJ, Krssak M, Kautschitsch S, Sommergruber W, Tontsch-Grunt U, et al. BIBF 1120: triple angiokinase inhibitor with sustained receptor blockade and good antitumor efficacy. Cancer Res 2008;68:4774–82.
30. Huynh H, Ngo VC, Fargnoli J, Ayers M, Soo KC, Koong HN, et al. Brivanib alaninate, a dual inhibitor of vascular endothelial growth factor receptor and fibroblast growth factor receptor tyrosine kinases, induces growth inhibition in mouse models of human hepatocellular carcinoma. Clin Cancer Res 2008;14:6146–53.
31. Sarker D, Molife R, Evans TR, Hardie M, Marriott C, Butzberger-Zimmerli P, et al. A phase I pharmacokinetic and pharmacodynamic study of TKI258, an oral, multitargeted receptor tyrosine kinase inhibitor in patients with advanced solid tumors. Clin Cancer Res 2008;14:2075–81.
32. Cabebe E, Wakelee H. Role of anti-angiogenesis agents in treating NSCLC: focus on bevacizumab and VEGFR tyrosine kinase inhibitors. Curr Treat Options Oncol 2007;8:15–27.
33. Folkman J. Angiogenesis: an organizing principle for drug discovery? Nat Rev Drug Discov 2007;6:273–86.
34. Herbst RS. Toxicities of antiangiogenic therapy in non-small-cell lung cancer. Clin Lung Cancer 2006;8 Suppl 1:S23–30.
35. Izzedine H, Ederhy S, Goldwasser F, Soria JC, Milano G, Cohen A, et al. Management of hypertension in angiogenesis inhibitor-treated patients. Ann Oncol 2009;20:807–15.
36. Ricciardi S, Tomao S, de Marinis F. Toxicity of targeted therapy in non-small-cell lung cancer management. Clin Lung Cancer 2009;10:28–35.
37. Shojaei F, Ferrara N. Role of the microenvironment in tumor growth and in refractoriness/resistance to anti-angiogenic therapies. Drug Resist Update 2008;11:219–30.
38. Gómez-Román JJ, Saenz P, Molina M, Cuevas González J, Escuredo K, Santa Cruz S, et al. Fibroblast growth factor receptor 3 is overexpressed in urinary tract carcinomas and modulates the neoplastic cell growth. Clin Cancer Res 2005;11:459–65.
39. Hara T, Ooi A, Kobayashi M, Mai M, Yanagihara K, Nakanishi I. Amplification of c-myc, K-sam, and c-met in gastric cancers: detection by fluorescence *in situ* hybridization. Lab Invest 1998;78: 1143–53.
40. Grand EK, Chase AJ, Heath C, Rahemtulla A, Cross NC. Targeting FGFR3 in multiple myeloma: inhibition of t(4;14)-positive cells by SU5402 and PD173074. Leukemia 2004;18:962–6.
41. Qian S, Somlo G, Zhou B, Yen Y. Therapeutic effects of thalidomide in myeloma are associated with the expression of fibroblast growth factor receptor 3. Ther Clin Risk Manag 2005;1:231–41.
42. Ogawa T, Takayama K, Takakura N, Kitano S, Ueno H. Anti-tumor angiogenesis therapy using soluble receptors: enhanced inhibition of tumor growth when soluble fibroblast growth factor receptor-1 is used with soluble vascular endothelial growth factor receptor. Cancer Gene Ther 2002;9:633–40.
43. Sepp-Lorenzino L, Rands E, Mao X, Connolly B, Shipman J, Antanavage J, et al. A novel orally bioavailable inhibitor of kinase insert domain-containing receptor induces antiangiogenic effects and prevents tumor growth *in vivo*. Cancer Res 2004;64:751–6.
44. Ronchetti D, Greco A, Compasso S, Colombo G, Dell'Era P, Otsuki T, et al. Deregulated FGFR3 mutants in multiple myeloma cell lines with t(4;14): comparative analysis of Y373C, K650E and the novel G384D mutations. Oncogene 2001;20:3553–62.
45. Finelli P, Fabris S, Zagano S, Baldini L, Intini D, Nobili L, et al. Detection of t(4;14)(p16.3;q32) chromosomal translocation in multiple myeloma by double-color fluorescent *in situ* hybridization. Blood 1999;94: 724–32.
46. Abdollahi A, Folkman J. Evading tumor evasion: current concepts and perspectives of anti-angiogenic cancer therapy. Drug Resist Updat 2010;13:16–28.
47. Ebos JM, Lee CR, Cruz-Munoz W, Bjarnason GA, Christensen JG, Kerbel RS. Accelerated metastasis after short-term treatment with a potent inhibitor of tumor angiogenesis. Cancer Cell 2009;15:232–9.
48. Pàez-Ribes M, Allen E, Hudock J, Takeda T, Okuyama H, Viñals F, et al. Antiangiogenic therapy elicits malignant progression of tumors to increased local invasion and distant metastasis. Cancer Cell 2009;15:220–31.